

Generation of flat temporal phase distribution of optical pulse by photonic crystal waveguides

Xin Lou (楼鑫)^{1,2*}, Yongming Nie (聂永名)^{1,2}, Jiali Liao (廖佳莉)^{2*},
Xuehua Yang (杨学华)¹, Puhua Huang (黄浦华)¹, Di Chen (陈迪)¹,
and Xiujian Li (李修建)²

¹China Satellite Maritime Tracking and Controlling Department,
Jiangyin 214431, China

²Science College, National University of Defense Technology,
Changsha 410073, China

*Corresponding author: 423307792@qq.com; 181895021@qq.com

Received July 29, 2013; accepted October 08, 2013; posted online March 20, 2014

We generate a flat temporal-phase distribution optical pulse by 1.3-mm-long photonic crystal waveguide. The effect of coupled pulse energy on the temporal-phase distribution of the output pulse is analyzed by numeral simulating. Simulation results indicate that the root mean square of the output pulse phase decreases to 0.0095 with the optimum coupled pulse energy, which is about 30 pJ, and the narrowest output pulse width is 418 fs. The generation of a flat temporal-phase distribution optical pulse on-chip scale results in potential application prospect in optical communication, pulse compression, pulse shaping and other nonlinear optical application fields.

OCIS codes: 320.0320, 190.4370, 060.0060.

doi: 10.3788/COL201412.S11903.

Solitons are ubiquitous. Since the first observation of soliton by J. S. Russell in the water of a shallow canal in 1834^[1], numerous examples of solitons have been observed in various physical, chemical, and biological environments, all propagating without spreading out or breaking up. Solitons of electromagnetic waves were even identified in an absolute vacuum^[2,3]. The technology of optical soliton generation has great value in the long-distance communication area and it has become the preferable scheme of new generation of the rapid velocity and long distance^[4]. The fascinating property of optical soliton has been attracting increasing interest in many fields, with potential applications ranging from optical amplification^[5], pulse compressing^[6,7], supercontinuum generation^[7-9], passive mode-locked lasers^[10] to optical switching and logical gating^[11-13]. The phase of the soliton has been extensively investigated from the phase noise to phase statistical properties, which play a significant role in the optical high-speed communication system^[14-16]. With the advantage of using a much higher group velocity dispersion (GVD) coefficient and nonlinear parameter γ of the photonic crystal waveguide (PCW) compared with those of the optical fiber and nanowire waveguide^[17-19], the optical solitons can be generated as several millimeter-long PCW, which is the most important step in demonstrating soliton dynamics on-chip scale. Here, we have used PCW to generate flat temporal-phase distribution, which is important information of optical solitons.

The flat temporal-phase distribution indicates that the chirp caused by self-phase modulation (SPM) balance with that caused by GVD^[20]. The effect of coupled pulse energy (Ep) on the phase of pulse propagating through PCW is analyzed by numerical simulation because the effect is significant, and the generation

of flat temporal-phase distribution depends on the well-controlled coupled pulse energy, while other parameters are determined by the PCW sample. The flat degree of the output pulse phase was evaluated by calculating the root mean square (RMS) of the phase distribution.

The electromagnetic wave propagation is governed by nonlinear Schrödinger equation (NLSE) in the PCW. The NLSE is expressed as follows^[20]

$$\begin{aligned} & \frac{\partial A}{\partial z} + \frac{1}{2} \alpha A + \frac{i\beta_2}{2} \frac{\partial^2 A}{\partial t^2} - \frac{\beta_3}{6} \frac{\partial^3 A}{\partial t^3} \\ & = i\gamma \left[|A|^2 A + \frac{2i}{\omega_0} \frac{\partial}{\partial T} (|A|^2 A) - T_R A \frac{\partial |A|^2}{\partial T} \right]. \end{aligned} \quad (1)$$

The two-photon absorption (TPA) by 1.9-eV band gap of GaInP^[2], which is much higher than the two-photon energy of the input pulse, can be suppressed, while the free-carrier absorption (FCA) can also be suppressed as a result of the relationship between the TPA coefficient with the FCA coefficient^[21,22]. The pulse width, in this paper, is about 5 ps to several hundred femtoseconds, thus the parameters $(\omega_0 T_0)^{-1}$ and Γ_R/T_0 become so small that the last two terms in Eq. (1) can be neglected^[20]. When the third-order dispersion is neglected for the coefficient of third-order dispersion, β_3 becomes much smaller than the GVD coefficient β_2 for the PCW used in this paper^[19]. The NLSE is simplified

$$\frac{\partial A}{\partial z} + \frac{1}{2} \alpha A + \frac{i\beta_2}{2} \frac{\partial^2 A}{\partial t^2} = i\gamma |A|^2 A. \quad (2)$$

The numerical simulation is based on the NLSE, above which is solved by split-step Fourier method using a 1.551- μm wavelength and 5-ps width input pulse

coupled with a 1.3-mm-long PCW. Other main parameters used in the numerical simulation are presented in this paper. The GVD coefficient and the nonlinear parameter are $0.91 \text{ ps}^2/\text{m}$ and 710 W/m , respectively, and the linear loss is 1 dB/mm , while the group index (n_g) is $8.3^{[19]}$.

The coupled pulse energy is increased from 18 to 34 pJ in the numerical simulation. The energy and phase of the output pulse are showed separately in Figs. 1 and 2. It is observed in these figures that the output pulse shapes in case of gradually changing E_p are completely different, and the phase of output pulse shifts sharply with the change in E_p . We have calculated the RMS of the output pulse phase to demonstrate the generation of flat temporal-phase distribution.

The peak intensity of the output pulse increases with the increase in E_p , and it reaches top with about 30 pJ coupled pulse energy. At the same time, the pulse width becomes narrow with an increase in E_p .

We pay attention only to the area of the output pulse width. Approximate flat property can be noticed easily. The phase shifts sharply at the edge of the pulse result from the numerical simulation method.

The data in Table 1 summarize the results of numerical simulation appropriately. Width is the temporal width of output pulse, and RMS describes the flat degree of the output pulse phase. The pulse width is

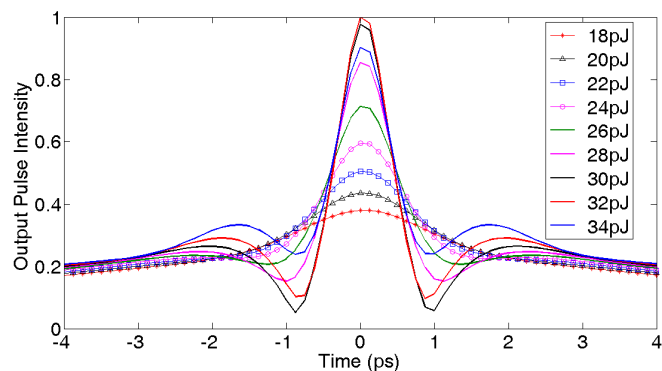


Fig. 1. Normalized intensity of output pulse with different coupled pulse energy.

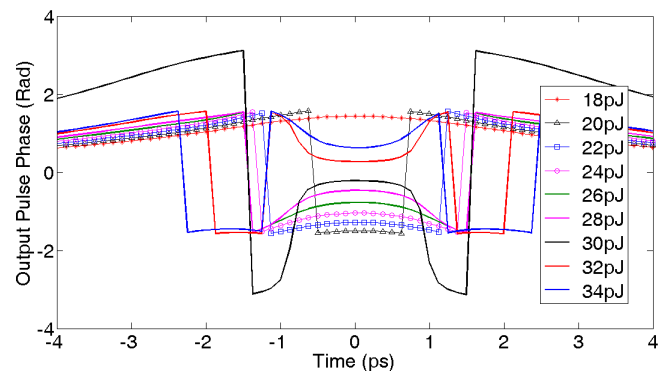


Fig. 2. The phase of output pulse with different coupled pulse energy.

Table 1. Results of the numerical simulation

E_p (pJ)	Width (fs)	RMS
18	1230	0.0656
20	1252	2.6993
22	953	0.0438
24	884	0.0570
26	557	0.0222
28	557	0.0217
30	418	0.0095
32	418	0.0154
34	418	0.0335

compressed through the short PCW, and the compression of pulse width is important when the coupled pulse energy increases to 30 pJ and the RMS of output pulse phase decreases to 0.0095 synchronously. Very small phase distribution RMS helps generate a flat temporal phase pulse, which indicates the balance between the SPM and the GVD. The RMS increases with increase in the coupled pulse energy more than 30 pJ, though the output pulse width is still 418 fs with the unbalance of the chirps due to SPM and GVD. A significant RMS with 20 pJ coupled pulse energy results from the sharp variety at the pulse edge, which can be observed in Figs. 1 and 2.

In conclusion, a flat temporal-phase distribution pulse is generated by 1.3-mm-long PCW. The intensity and the phase of the output pulse are analyzed by numerical simulation by varying the coupled pulse energy (E_p). The RMS of the output pulse phase decreases to 0.0095 with optimum E_p , which is about 30 pJ, and the output pulse width is 418 fs, which is the narrowest among different cases. The generation of a flat temporal-phase distribution pulse on-chip scale results in potential applications in pulse compression, pulse shaping, optical communication and other nonlinear optical application fields.

This research was funded by the National Natural Science Foundation of China (NSFC) under no. 60907003, no. 61070040 and no. 60673147.

References

1. J. S. Russell, in *Reports of the Meetings of the British Association for the Advancement of Science, 1844, Liverpool Meeting* (1838).
2. M. Segev, *Opt. Photon. News* **13**, 27 (2002).
3. B. L. Mantsyzov, I. V. Silnikov, and J. S. Aitchison, *IEEE J. Sel. Top. Quantum Electron* **10**, 893 (2004).
4. H. A. Haus and W. S. Wong, *Rev. Mod. Phys.* **68**, 423 (1996).
5. W. H. Renninger, A. Chong, and F. W. Wise, *Opt. Lett.* **33**, 3025 (2008).
6. X. Zeng, H. Guo, B. Zhou, and M. Bache, *Opt. Express* **20**, 27072 (2012).
7. M. A. Foster and A. L. Gaeta, *Opt. Express* **13**, 6848 (2005).

8. L. H. Yin, Q. Lin, and G. P. Agrawal, *Opt. Lett.* **32**, 391 (2007).
9. E. J. R. Kelleher, M. Erkintalo, and J. C. Travers, *Opt. Lett.* **37**, 5217 (2012).
10. P. Grelul and N. Akhmediev, *Nat. Photo.* **6**, 84 (2012).
11. M. Peccianti, C. Conti, G. Assanto, A. D. Luca, and C. Umeton, *Appl. Phys. Lett.* **81**, 3335 (2002).
12. M. Peccianti, C. Conti, G. Assanto, A. D. Luca, and C. Umeton, *Nature* **432**, 733 (2004).
13. R. McLeod, K. Wagner, and S. Blair, *Phys. Rev. A.* **52**, 3254 (1995).
14. L. Jankovic, S. Polyakov, G. Stegeman, S. Carrasco, L. Torner, C. Bosshard, and P. Gunter, *Opt. Express* **11**, 2206 (2003).
15. R. Essiambre and G. P. Agrawal, *J. Opt. Soc. Am. B.* **14**, 323 (2007).
16. K. Po Ho, *J. Opt. Soc. Am. B.* **21**, 266 (2004).
17. J. Zhang, Q. Lin, G. Piredda, R. W. Boyd, G. P. Agrawal, and P. M. Fauchet, *Opt. Express* **15**, 7682 (2007).
18. K. Chan and W. Cao, *J. Opt. Soc. Am. B.* **15**, 2371 (1998).
19. P. Colman, C. Husko, S. Combrie, I. Sagnes, C. W. Wong, and A. De Rossi, *Nat. Photo.* **4**, 862 (2010).
20. Q. Lin, O. J. Painter, and G. P. Agrawal, *Opt. Express* **15**, 16604 (2007).
21. H. Garcia and R. Kalyanaraman, *J. Phys. B: At. Mol. Opt. Phys.* **39**, 2737 (2006).
22. A. C. Turner-Foster, M. A. Foster, J. S. Levy, C. B. Poitras, R. Salem, A. L. Gaeta, and M. Lipson, *Opt. Express* **18**, 3582 (2010).